Receive Quadrature Reflecting Modulation for RIS-Empowered Wireless Communications

Jing Yuan, Miaowen Wen, *Senior Member, IEEE*,
Qiang Li, *Member, IEEE*, Ertugrul Basar, *Senior Member, IEEE*,
George C. Alexandropoulos, *Senior Member, IEEE*,
and Gaojie Chen, *Senior Member, IEEE*

Abstract—In this paper, we propose a novel reconfigurable intelligent surface (RIS)-based modulation scheme, named RIS-aided receive quadrature reflecting modulation (RIS-RQRM), by resorting to the concept of spatial modulation. In RIS-RQRM, the whole RIS is virtually partitioned into two halves to create signals with only in-phase (I-) and quadrature (Q-) components, respectively, and each half forms a beam to a receive antenna whose index carries the bit information. Furthermore, we design a low-complexity and non-coherent detector for RIS-RQRM, which measures the maximum power and polarities of the I- and Q- components of received signals. Approximate bit error rate (BER) expressions are derived for RIS-RQRM over Rician fading channels. Simulation results show that RIS-RQRM outperforms the existing counterparts without I/Q index modulation in terms of BER in the low signal-to-noise ratio region.

Index Terms—Reconfigurable intelligent surface (RIS), spatial modulation, bit error rate, reflection modulation.

I. INTRODUCTION

Owing to their capability of making the environment controllable, reconfigurable intelligent surfaces (RISs) have been recently attracting considerable attention [1]. An RIS comprises a large number of reflecting elements, each of which is able to reflect the incident waves with an adjustable reflection coefficient. By intentionally controlling the reflection characteristics of incident waves, RISs can achieve different purposes, such as transmit power minimization [2], error performance improvement [3], and energy efficiency enhancement [4]. Actually, by configuring the reflection coefficients according to the information to be transmitted, RISs can also be employed for information transfer, creating the concept of RIS-based modulation. It was shown in [5] that an RIS-based multiple-input multiple-output transmitter can be built by illuminating an RIS with an unmodulated carrier signal and performing phase shift keying (PSK)/quadrature amplitude modulation (QAM) at

each reflecting element according to the source data. Moreover, by jointly optimizing the on-off situation and reflection coefficients of elements, the error performance of an RIS-based system can be highly improved [6], [7]. It is thus apparent that RISs enhance the performance of existing communication systems, and provide numerous opportunities for designing new modulation schemes.

Spatial modulation (SM), which activates a single transmit antenna per transmission and exploits the index of the active antenna to carry spatial bits, is also an innovative digital modulation technology [8]. Earlier, SM has been combined with traditional communication technologies. For instance, the authors of [9] proposed an SM aided non-orthogonal multiple access (NOMA) with full-duplex relay scheme to improve the ergodic capacity and bit error rate (BER) by combining SM with NOMA and relaying. Recently, the ideas of SM and its variants have been introduced into RIS-based systems, resulting in three RIS-based SM communication scenarios, in which the SM concept is applied to the transmitter-side, to the RIS, and to the receiver-side, respectively [10]. As RIS-based SM at the receiver-side, RIS-SM and RIS-SSK employ RIS-based passive beamforming instead of active pre-coding to steer the signal towards a certain receive antenna. The RIS-based SM at the RIS was investigated in [11]–[13]. In [11] and [12], not all reflecting elements were activated, and the positions of the active elements were determined by the information to be transmitted. In [13], all reflecting elements were activated, and the index of a reflection coefficient pattern conveys information per channel use.

In this paper, inspired by the receive quadrature SM (RQSM) concept, we propose a novel RIS-based modulation scheme, termed RIS-aided receive quadrature reflecting modulation (RIS-RQRM). The contributions of this paper are summarized as follows.

- The technologies of RISs and RQSM are amalgamated for the first time. In RIS-RQRM, the RIS is partitioned into two halves to create signals with only in-phase (I-) and quadrature (Q-) components, respectively. The I- and Q- components of a reflected signal are steered to two receive antennas separately, whose indices carry two different data streams. Compared with RQSM, RIS-RQRM does not transmit constellation symbols, but enables two more spatial bits to be conveyed for determining the polarities of the I- and Q- parts.

- A low-complexity detector is developed for RIS-RQRM, which measures the maximum power and polarities of the I- and Q- components of received signals, and dispenses with the channel state information (CSI) at the receiver. The resulting BER performance of RIS-RQRM over Rician fading channels is investigated, and approximate average bit error probability (ABEP) expressions are derived. Simulation results show that RIS-RQRM outperforms RIS-SSK and RIS-SM [10] in terms of BER in the low SNR region.

Notation: $\mathbb{C}^{m \times n}$ denotes the space of $m \times n$ complex-valued matrices. $j = \sqrt{-1}$ is the imaginary unit. $|\cdot|$ and $C(\cdot, \cdot)$ denote the modulus/absolute value and the binomial coefficient, respectively. The real part of a complex number is denoted by $(\cdot)_\Re$. $(\mathcal{C})\mathcal{N}(\mu, \sigma^2)$ represents the (complex) Gaussian distribution with mean μ and variance σ^2. The probability of an event and the probability density function of a random variable are denoted by $\Pr(\cdot)$ and $f(\cdot)$, respectively. $Q_1(\cdot)$ and I_0 represent the first order Marcum Q-function and the zeroth-order modified Bessel function of the first kind, respectively [14]. The cumulative distribution function of the standard normal distribution is denoted by $\Phi(\cdot)$.

Jing Yuan and Miaowen Wen are with the School of Electronic and Information Engineering, South China University of Technology, Guangzhou 510640, China (e-mail: eeyj@mail.scut.edu.cn; eemwwen@scut.edu.cn).

Qiang Li is with the College of Information Science and Technology, Jinan University, Guangzhou 510632, China (e-mail: qiangli@jnu.edu.cn).

Ertugrul Basar is with the CoreLab, Department of Electrical and Electronics Engineering, Koç University, Istanbul 34450, Turkey (e-mail: ebasar@ku.edu.tr).

George C. Alexandropoulos is with the Department of Informatics and Telecommunications, National and Kapodistrian University of Athens, 15784 Panepistimiopolis Ilissia, Athens Greece (e-mail: alexandg@ieee.org).

Gaojie Chen is with the School of Engineering, University of Leicester, LE1 7HB Leicester, U.K. (e-mail: Gaojie.Chen@leicester.ac.uk).
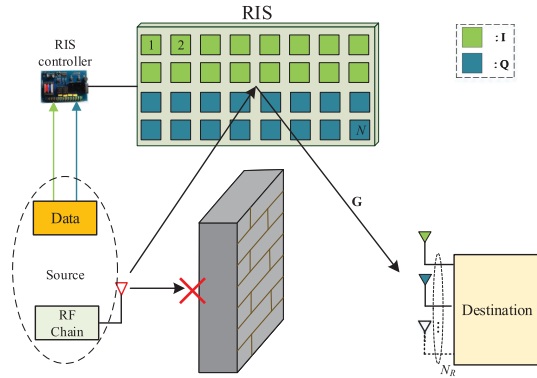
Fig. 1.   System model of RIS-RQRM.

II. SYSTEM MODEL

Fig. 1 illustrates the considered system model, which comprises a single-antenna radio frequency (RF) source, an N-element RIS, and an N_R-antenna destination, where $N, N_R \geq 2$. Due to an obstacle, there is no direct link between the RF source and the destination. The RF source transmits an unmodulated carrier signal, and the RIS reflects the signal in a deliberate manner to convey information bits. In this paper, since the RIS is close to the RF source, and thus considered as a part of the transmitter, we ignore the fading effects between the RF source and the RIS [10]. Let $\mathbf{G} \in \mathbb{C}^{N_R \times N}$ denotes the channel matrix between the RIS and the destination. We assume that all channel links from the RIS to the destination are independent of each other and experience quasi-static flat Rician fading. The (l, i)th entry of $\mathbf{G}$ can be expressed as

$$g_{l,i} = \sqrt{\frac{K}{K+1}}\bar{g}_{l,i} + \sqrt{\frac{1}{K+1}}\tilde{g}_{l,i} = |g_{l,i}|\exp\left(j\theta_{l,i}\right), \quad (1)$$

where $l \in \{1, \dots, N_R\}$, $i \in \{1, \dots, N\}$, $K \geq 0$ is the Rician factor, $\bar{g}_{l,i} \in \mathbb{C}$ with $|\bar{g}_{l,i}| = 1$ denotes the deterministic line-of-sight (LoS) component, and $\tilde{g}_{l,i} \in \mathbb{C}$ with $\tilde{g}_{l,i} \sim \mathcal{CN}(0,1)$ denotes the non-LoS component. The reflection coefficient for the ith reflecting element of the RIS is expressed as $c_i = \exp(j\alpha_i)$, where α_i is continuously varied over $[0, 2\pi)$.

A. Principle of RIS-RQRM

For the proposed RIS-RQRM, the RIS is randomly partitioned into two halves, each containing $N/2$ reflecting elements. The information bits to be transmitted are also divided into two parts (corresponding to the I- and Q- branches), with each containing $n + 1$ bits. Through the RIS controller, the I- and Q- branches control the two halves of the RIS, respectively. For the I-branch, the first $n = \log_2 N_R$[1] bits determine the index of the receive antenna that the I-component of the reflected signal targets, say $m_1 \in \{1, \dots, N_R\}$. The last one bit, denoted by $d_I \in \{0, 1\}$, determines the positive/negative polarity of the beam of the I-component. Similarly, for the Q-branch, the index of the targeted receive antenna and the polarity bit of the Q-component are denoted by $m_2 \in \{1, \dots, N_R\}$ and $d_Q \in \{0, 1\}$, respectively. Therefore, the reflection coefficients for elements controlled by the I- and Q- branches can be expressed as

$$c_i = (-1)^{d_I}\exp\left(-j\theta_{m_1,i}\right), \quad i = 1, \dots, N/2 \quad (2)$$

[1] In this paper, N_R is assumed to be an arbitrary integer power of two. m_1 and m_2 can be easily obtained by converting the corresponding n bits into the decimal representation.

and

$$c_i = j(-1)^{d_Q}\exp\left(-j\theta_{m_2,i}\right), \quad i = N/2 + 1, \dots, N, \quad (3)$$

respectively. The received signal at the lth receive antenna can be expressed as

$$y_l = (-1)^{d_I}\sum_{i=1}^{N/2}|g_{l,i}|\exp\left(j\left(\theta_{l,i} - \theta_{m_1,i}\right)\right)$$

$$+ j(-1)^{d_Q}\sum_{i=N/2+1}^{N}|g_{l,i}|\exp\left(j\left(\theta_{l,i} - \theta_{m_2,i}\right)\right) + n_l, \quad (4)$$

where n_l is the additive white Gaussian noise at the lth receive antenna following $\mathcal{CN}(0, N_0)$.

As depicted above, a unique reflecting pattern is created for each channel use according to the information bits. Consequently, the I- and Q- components of the reflected signal are polarized and steered to two specific receive antennas, respectively. As seen from (4), with $l = m_1$ ($l = m_2$), the I (Q)-component of the received signal at the antenna selected by the I (Q)-branch is the sum of $N/2$ sub-channels with the same phase. Therefore, it is more probable that the power is larger than that of any other receive antennas.

B. Low-Complexity and Non-Coherent Receiver

As the decoding process for the I- and Q- branches are independent, we only take the I-branch as an illustrative example. According to the beamforming principle mentioned above, the power of the I-component of the received signal at the m_1th receive antenna is supposed to be higher than that of any other receive antennas, that is

$$\hat{m}_1 = \arg\max_l \left|(y_l)_\Re\right|, \quad (5)$$

where $\hat{m}_1$ is the estimate of m_1. After obtaining $\hat{m}_1$, the estimate of d_I, denoted by $\hat{d}_I$, can be easily derived from

$$\hat{d}_I = \begin{cases} 0, & (y_{\hat{m}_1})_\Re \geq 0, \\ 1, & (y_{\hat{m}_1})_\Re < 0. \end{cases} \quad (6)$$

We observe from (5) and (6) that the detector enjoys low detection complexity and dispenses with the CSI at the receiver.

Remark 1: The RIS-RQRM can be extended to the scenario where a constellation symbol is transmitted from the RF source. However, the phase-related modulation schemes, e.g. PSK and QAM will misdirect the signals. In order to avoid phase ambiguity, the constellation symbol is restricted to an M-ary pulse amplitude modulation (PAM) symbol on the I-dimension. The Q-branch works as in the absence of the M-PAM modulator. For the I-branch, since the PAM symbol itself introduces a phase shift of π, d_I should be fixed, which results in a loss of 1-bit spatial information. In this case, the spectral efficiency becomes $2\log_2 N_R + \log_2 M + 1$ bits per channel use.

III. PERFORMANCE ANALYSIS

In this section, we analyze the ABEPs of RIS-RQRM utilizing the detector in (5) and (6). Due to symmetry, we will elaborate only on the I-branch in the following.

Obviously, the error events can be classified into two complementary types, depending on whether $m_1 = m_2$ or not. Thus, the ABEP can be evaluated as

$$P_b = R_1 P_{b1} + R_2 P_{b2}, \quad (7)$$

where $R_1 = 1/N_R$ and $R_2 = (N_R - 1)/N_R$ denote the possibilities of $m_1 = m_2$ and $m_1 \neq m_2$, respectively; P_{b1} and P_{b2} are the ABEPs for the cases of $m_1 = m_2$ and $m_1 \neq m_2$, respectively. In the next two subsections, we will present the derivations of P_{b1} and P_{b2}, respectively.

A. Calculation of P_{b1}

In this case, by substituting $l = m_1 = m_2 = m$ and $l = \bar{m}$ into (4), we have y_m and $y_{\bar{m}}$. Obviously, the probability of detecting m erroneously can be evaluated as [15, Eq. (24)]

$$P_{im} = 1 - \Pr\left(\bigcap_{\substack{\bar{m}=1 \\ \bar{m} \neq m}}^{N_R} |(y_{\bar{m}})_\Re| \leq |(y_m)_\Re|\right)$$

$$\approx 1 - \prod_{\bar{m}=1, \bar{m}\neq m}^{N_R} \Pr\left(|B_1| \leq |A_1|\right), \qquad (8)$$

where $A_1 = (y_m)_\Re$, $B_1 = (y_{\bar{m}})_\Re$, and the approximation results from the assumption that the signals at different receive antennas are statistically independent of each other. It can be shown that the distribution of $|A_1|$ is irrelevant to d_I and d_Q, while that of $|B_1|$ depends on whether $d_I = d_Q$ or not. Let us take $d_I = d_Q = 0$ as an example. Conditioned on $\mathbf{G}$ and $d_I = d_Q = 0$, we have $A_1 \sim \mathcal{N}(E_{A_1}, N_0/2)$ and $B_1 \sim \mathcal{N}(E_{B_1}, N_0/2)$, where $E_{A_1} = \sum_{i=1}^{N/2} |g_{m,i}|$ and

$$E_{B_1} = \left(\sum_{i=1}^{N/2} |g_{\bar{m},i}| \exp\left(j\left(\theta_{\bar{m},i} - \theta_{m,i}\right)\right)\right.$$

$$\left. + j \sum_{i=N/2+1}^{N} |g_{\bar{m},i}| \exp\left(j\left(\theta_{\bar{m},i} - \theta_{m,i}\right)\right)\right)_\Re.$$

Since $|B_1|^2 - |A_1|^2$ is a special quadratic form of complex Gaussian random variables, we have [14, Eq. (9 A.10)]

$$\Pr(|B_1|^2 < |A_1|^2 | \mathbf{G}, 00)$$

$$= Q_1(a, b) - \frac{1}{2} \exp\left(-\frac{a^2 + b^2}{2}\right) I_0(ab), \qquad (9)$$

where 00 denotes $d_I = d_Q = 0$ and

$$a = \sqrt{\frac{2v_1^2 v_2 \left(\xi_1 v_2 - \xi_2\right)}{(v_1 + v_2)^2}}, \quad b = \sqrt{\frac{2v_2^2 v_1 \left(\xi_1 v_1 + \xi_2\right)}{(v_1 + v_2)^2}},$$

$$v_1 = \sqrt{w^2 + \frac{1}{4u_{xx}u_{yy}}} - w, \quad v_2 = \sqrt{w^2 + \frac{1}{4u_{xx}u_{yy}}} + w,$$

$$\xi_1 = 2\left((E_{B_1})^2 u_{yy} + (E_{A_1})^2 u_{xx}\right), \quad \xi_2 = (E_{B_1})^2 - (E_{A_1})^2,$$

$$w = \frac{u_{xx} - u_{yy}}{4u_{xx}u_{yy}}, \qquad u_{xx} = \frac{N_0}{4}, \qquad u_{yy} = \frac{N_0}{4}.$$

Then, the error probability of detecting m conditioned on $\mathbf{G}$ and $d_I = d_Q = 0$, denoted by $P_{im|\mathbf{G},00}$, can be calculated by (8). Under this condition, the error probability of detecting d_I can be expressed as

$$P_{dm|\mathbf{G},00} = \Phi\left(\frac{-E_{A_1}}{\sqrt{N_0/2}}\right) \qquad (10)$$

and

$$P_{d\bar{m}|\mathbf{G},00} = \frac{1}{N_R - 1} \sum_{\substack{\bar{m}=1 \\ \bar{m}\neq m}}^{N_R} \Phi\left(\frac{-E_{B_1}}{\sqrt{N_0/2}}\right) \qquad (11)$$

for the cases where m is detected correctly and incorrectly, respectively.

Finally, by considering all possible events in the detection process, P_{b1} conditioned on $\mathbf{G}$ and $d_I = d_Q = 0$ is given by

$$P_{b1|\mathbf{G},00} = \frac{1}{n+1} \left[\left(1 - P_{im|\mathbf{G},00}\right) P_{dm|\mathbf{G},00}\right.$$

$$+ P_{im|\mathbf{G},00}(1 - P_{d\bar{m}|\mathbf{G},00})d_m$$

$$\left. + P_{im|\mathbf{G},00}P_{d\bar{m}|\mathbf{G},00}(1 + d_m)\right], \qquad (12)$$

where d_m is the average number of erroneous bits when m is detected incorrectly. Since m may be detected incorrectly as one of the remaining $N_R - 1$ indices with equal probability, and the number of erroneous bits ranges from 1 to n, d_m can be derived as

$$d_m = \frac{1}{N_R - 1} \sum_{x=1}^{n} xC(n, x) = \frac{N_R \log_2 N_R}{2(N_R - 1)}. \qquad (13)$$

Similarly, we can obtain P_{b1} conditioned on $\mathbf{G}$ and $d_I \neq d_Q$. Here, we consider $d_I = 0$ and $d_Q = 1$ without loss of generality. Therefore, the conditional P_{b1} can be evaluated as

$$P_{b1|\mathbf{G}} = \frac{1}{2}\left(P_{b1|\mathbf{G},00} + P_{b1|\mathbf{G},01}\right). \qquad (14)$$

B. Calculation of P_{b2}

In this case, $m_1 \neq m_2$ and m_1 may be erroneously detected as m_2 or m_3 ($m_3 \neq m_1$ and $m_3 \neq m_2$). Let us define $A_2 = (y_{m_1})_\Re$, $B_2 = (y_{m_2})_\Re$, and $C_2 = (y_{m_3})_\Re$. Similar to the derivation of P_{b1}, we only need to discuss the cases where $d_I = d_Q = 0$ and $d_I = 0, d_Q = 1$. Conditioned on $\mathbf{G}$ and $d_I = d_Q = 0$, we have $A_2 \sim \mathcal{N}(E_{A_2}, N_0/2)$, $B_2 \sim \mathcal{N}(E_{B_2}, N_0/2)$, and $C_2 \sim \mathcal{N}(E_{C_2}, N_0/2)$, where

$$E_{A_2} = \sum_{i=1}^{N/2} |g_{m_1,i}|$$

$$+ \left(j \sum_{i=N/2+1}^{N} |g_{m_1,i}| \exp\left(j\left(\theta_{m_1,i} - \theta_{m_2,i}\right)\right)\right)_\Re,$$

$$E_{B_2} = \left(\sum_{i=1}^{N/2} |g_{m_2,i}| \exp\left(j\left(\theta_{m_2,i} - \theta_{m_1,i}\right)\right)\right)_\Re,$$

and

$$E_{C_2} = \left(\sum_{i=1}^{N/2} |g_{m_3,i}| \exp\left(j\left(\theta_{m_3,i} - \theta_{m_1,i}\right)\right)\right.$$

$$\left. + j \sum_{i=N/2+1}^{N} |g_{m_3,i}| \exp\left(j\left(\theta_{m_3,i} - \theta_{m_2,i}\right)\right)\right)_\Re.$$

Resorting to (9), we can obtain $\Pr(|B_2|^2 < |A_2|^2 | \mathbf{G}, 00)$ and $\Pr(|C_2|^2 < |A_2|^2 | \mathbf{G}, 00)$. The probability of detecting m_1 correctly conditioned on $\mathbf{G}$ and $d_I = d_Q = 0$ can be given by

$$P_{im_1|\mathbf{G},00} \approx \Pr\left(|B_2|^2 \leq |A_2|^2 | \mathbf{G}, 00\right)$$

$$\times \prod_{\substack{m_3=1 \\ m_3\neq m_1, m_3\neq m_2}}^{N_R} \Pr\left(|C_2|^2 \leq |A_2|^2 | \mathbf{G}, 00\right). \qquad (15)$$

Similarly, we can obtain the conditional probability of detecting m_1 incorrectly as m_2, which is denoted by $P_{im_2|\mathbf{G},00}$.

When m_1 is detected correctly, the error probability of detecting d_I is

$$P_{dm_1|\mathbf{G},00} = \Phi\left(\frac{-E_{A_2}}{\sqrt{N_0/2}}\right). \quad (16)$$

By contrast, when m_1 is detected erroneously as m_2 and m_3, the error probabilities of detecting d_I can be evaluated as

$$P_{dm_2|\mathbf{G},00} = \Phi\left(\frac{-E_{B_2}}{\sqrt{N_0/2}}\right) \quad (17)$$

and

$$P_{dm_3|\mathbf{G},00} = \frac{1}{N_R-2} \sum_{\substack{m_3=1 \\ m_3\neq m_1, m_3\neq m_2}}^{N_R} \Phi\left(\frac{-E_{C_2}}{\sqrt{N_0/2}}\right), \quad (18)$$

respectively.

By analyzing all possible error events, we have

$$P_{b2|\mathbf{G},00} = \frac{1}{n+1}$$
$$\times \left[P_{im_1|\mathbf{G},00} P_{dm_1|\mathbf{G},00} + P_{im_2|\mathbf{G},00} \left(1 - P_{dm_2|\mathbf{G},00}\right) h \right.$$
$$+ P_{im_2|\mathbf{G},00} P_{dm_2|\mathbf{G},00} (h+1)$$
$$+ \left(1 - P_{im_1|\mathbf{G},00} - P_{im_2|\mathbf{G},00}\right)\left(1 - P_{dm_3|\mathbf{G},00}\right) d_h$$
$$\left. + \left(1 - P_{im_1\mathbf{G},00} - P_{im_2|\mathbf{G},00}\right) P_{dm_3|\mathbf{G},00} (d_h+1)\right],$$

where h is the number of erroneous bits when m_1 is detected as m_2, and d_h is the average number of erroneous bits when m_1 is detected as m_3, i.e.,

$$d_h = \begin{cases} 0, & N_R = 2 \\ \frac{1}{N_R-2}\left(\frac{1}{2}N_R\log_2 N_R - h\right), & N_R > 2. \end{cases} \quad (19)$$

Similarly, we can obtain $P_{b2|\mathbf{G},01}$ conditioned on $\mathbf{G}$, $d_I = 0$, and $d_Q = 1$. Then, we have $P_{b2|\mathbf{G}} = (P_{b2|\mathbf{G},00} + P_{b2|\mathbf{G},01})/2$. After obtaining $P_{b1|\mathbf{G}}$ and $P_{b2|\mathbf{G}}$, $P_{b|\mathbf{G}}$ can be derived via (7). Finally, averaging $P_{b|\mathbf{G}}$ over $\mathbf{G}$ via numerical evaluation leads to P_b.

Remark 2: When $K = 0$, $g_{l,i}$ follows $\mathcal{CN}(0,1)$. By resorting to the central limit theorem, it can be deduced that

$$A_1 \sim \mathcal{N}\left(\frac{N\sqrt{\pi}}{4}, \frac{N(4-\pi)}{8} + \frac{N_0}{2}\right),$$

$$A_2 \sim \mathcal{N}\left(\frac{N\sqrt{\pi}}{4}, \frac{N(6-\pi)}{8} + \frac{N_0}{2}\right),$$

$$B_1, C_2 \sim \mathcal{N}\left(0, \frac{N+N_0}{2}\right) \text{ and } B_2 \sim \mathcal{N}\left(0, \frac{N+2N_0}{4}\right),$$

which are all irrelevant to d_I and d_Q. Then, (9) can be calculated by

$$\Pr(|Y| \leq |X|) = 2\int_0^{+\infty} f_Y(y) \int_{-y}^{y} f_X(x)\mathrm{d}x\mathrm{d}y. \quad (20)$$

The result of (20) can be easily attained by mathematical software such as MATLAB through numerical integration.
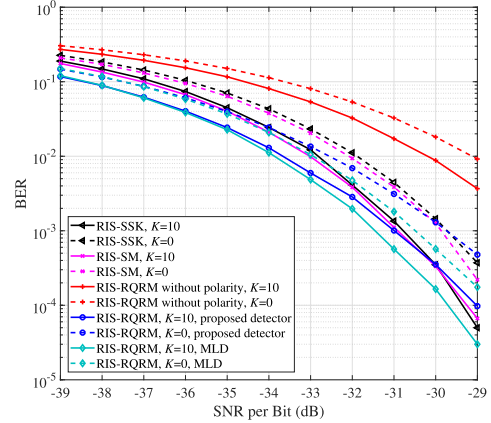

Fig. 2. Performance comparison among RIS-RQRM, RIS-SSK, and RIS-SM with QPSK, where $N_R = 2$, $N = 128$, and $K = 0$ and 10.
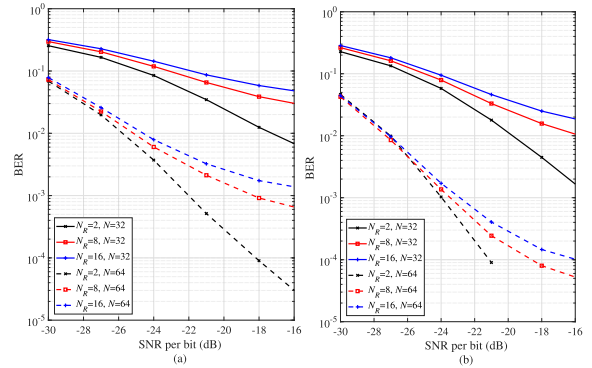

Fig. 3. Performance of RIS-RQRM for (a) $K = 0$ and (b) $K = 10$, where $N_R = 2, 8$, and 16, and $N = 32$ and 64.

IV. SIMULATION RESULTS

In this section, the BER performance of RIS-RQRM over Rician fading channels is assessed through Monte Carlo simulations. To demonstrate the superiority over conventional schemes, we make comparisons between RIS-RQRM and RIS-SSK as well as RIS-SM [10], both of which employ non-coherent detectors. The comparison between the proposed detector and ML detector is also made. As a special case, the RIS-RQRM scheme without polarity bits is also taken as a benchmark. We plot the BER versus transmit SNR per bit and neglect any large-scale path loss effect.

Fig. 2 shows the BER curves of RIS-RQRM, RIS-SSK, RIS-SM and RIS-RQRM without polarity bits, where $N_R = 2$, $N = 128$, and $K = 0$ and 10. The deterministic LoS components of the channel are all unit-modulus complex numbers. The symbol transmitted by RIS-SM is extracted from QPSK. As seen from Fig. 2, a larger K from 0 to 10 results in an SNR gain of about 1 dB for RIS-RQRM at a BER value of 10^{-3}. For both $K = 0$ and $K = 10$, RIS-RQRM outperforms RIS-RQRM without polarity throughout the considered SNR region. Particularly, the BER curve of RIS-RQRM intersects with that of RIS-SSK and RIS-SM, respectively. At low SNR, roughly less than -30 dB, RIS-RQRM performs better than RIS-SSK and RIS-SM. As seen from the results of RIS-RQRM with the proposed detector and the ML detector, the former is more practicable at low SNR due to its low complexity.
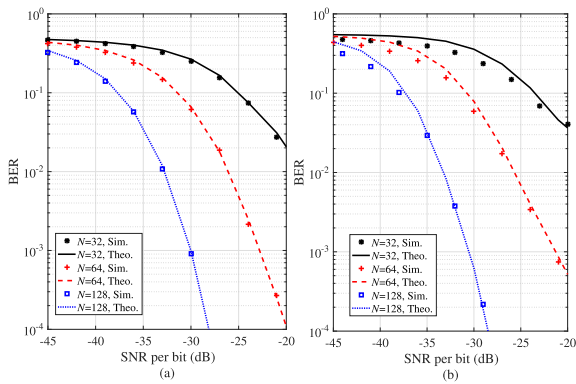
Fig. 4. Simulation and theoretical results of RIS-RQRM for (a) $N_R = 2$ and (b) $N_R = 4$, where $K = 1$, and $N = 32, 64,$ and 128.

Fig. 3 examines the impacts of N_R and N on the BER performance of RIS-RQRM, where $N_R = 2, 8$ and 16, $N = 32$ and 64, and $K = 0$ and 10 are considered. As seen from Fig. 3, increasing N significantly improves the BER performance of RIS-RQRM for both $K = 0$ and $K = 10$. This is because a larger value of N energizes the targeted receive antennas more powerfully. By contrast, increasing N_R deteriorates the performance, achieving the trade-off between spectral efficiency and BER performance.

Fig. 4 presents the simulated and theoretical BER curves of RIS-RQRM, where $N_R = 2$ and 4, $N = 32, 64,$ and 128 and $K = 1$. It can be seen from Fig. 4 that for $N_R = 2$, the theoretical curves agree with the simulated counterparts very well throughout the considered SNR region, while for $N_R = 4$, there is a small gap between a theoretical curve and its simulated counterpart due to the adopted approximations in the calculation of $P_{im|\mathbf{G},00}$, $P_{im_1|\mathbf{G},00}$, and $P_{im_2|\mathbf{G},00}$.

V. CONCLUSION

In this paper, RIS-RQRM was proposed by exploiting the concept of spatial modulation, where the RIS is divided into two halves. Each halve of elements is controlled by a data stream to form a beam to a receive antenna whose index carries the bit information. A low-complexity energy-based detector was designed for RIS-RQRM. Approximate mathematical expressions for the ABEPs of RIS-RQRM over Rician fading channels have been derived. Finally, the BER performance of RIS-RQRM was simulated extensively, whose results show that RIS-RQRM is superior to the existing RIS-SSK and RIS-SM in the low SNR region. The RIS-RQRM can be applied to single RF transmitter implementations, and we will devote to exploring more abundant application scenarios in the future.

REFERENCES

[1] E. Basar, M. Di Renzo, J. de Rosny, M. Debbah, M.-S. Alouini, and R. Zhang, "Wireless communications through reconfigurable intelligent surfaces," *IEEE Access*, vol. 7, pp. 116753–116773, 2019.

[2] Q. Wu and R. Zhang, "Intelligent reflecting surface enhanced wireless network via joint active and passive beamforming," *IEEE Trans. Wireless Commun.*, vol. 18, no. 11, pp. 5394–5409, Nov. 2019.

[3] J. Ye, S. Guo, and M.-S. Alouini, "Joint reflecting and precoding designs for SER minimization in reconfigurable intelligent surfaces assisted MIMO systems," *IEEE Trans. Wireless Commun.*, vol. 19, no. 8, pp. 5561–5574, Aug. 2020.

[4] C. Huang, A. Zappone, G. C. Alexandropoulos, M. Debbah, and C. Yuen, "Reconfigurable intelligent surfaces for energy efficiency in wireless communication," *IEEE Trans. Wireless Commun.*, vol. 18, no. 8, pp. 4157–4170, Aug. 2019.

[5] W. Tang *et al.*, "MIMO transmission through reconfigurable intelligent surface: System design, analysis, and implementation," *IEEE J. Sel. Areas Commun.*, vol. 38, no. 11, pp. 2683–2699, Nov. 2020.

[6] C. Pradhan, A. Li, L. Song, B. Vucetic, and Y. Li, "Hybrid precoding design for reconfigurable intelligent surface aided mmWave communication systems," *IEEE Commun. Lett.*, vol. 9, no 7, pp. 1041–1045, Jul. 2020.

[7] A. Li, L. Song, B. Vucetic, and Y. Li, "Interference exploitation precoding for reconfigurable intelligent surface aided multi-user communications with direct links," *IEEE Commun. Lett.*, vol. 9, no 11, pp. 1937–1941, Nov. 2020.

[8] M. Wen *et al.*, "A survey on spatial modulation in emerging wireless systems: Research progresses and applications," *IEEE J. Sel. Areas Commun.*, vol. 37, no. 9, pp. 1949–1972, Sep. 2019.

[9] Q. Si, M. Jin, Y. Chen, N. Zhao, and X. Wang, "Performance analysis of spatial modulation aided NOMA with full-duplex relay," *IEEE Trans. Veh. Technol.*, vol. 69, no. 5, pp. 5683–5687, May 2020.

[10] E. Basar, "Reconfigurable intelligent surface-based index modulation: A new beyond MIMO paradigm for 6 G," *IEEE Trans. Commun.*, vol. 68, no. 5, pp. 3187–3196, May 2020.

[11] W. Yan, X. Yuan, Z. He, and X. Kuai, "Passive beamforming and information transfer design for reconfigurable intelligent surfaces aided multiuser MIMO systems," *IEEE J. Sel. Areas Commun.*, vol. 38, no. 8, pp. 1793–1808, Aug. 2020.

[12] S. Lin, B. Zheng, G. C. Alexandropoulos, M. Wen, M. D. Renzo, and F. Chen, "Reconfigurable intelligent surfaces with reflection pattern modulation: Beamforming design and performance analysis," *IEEE Trans. Wireless Commun.*, vol. 20, no. 2, pp. 741–754, Feb. 2020.

[13] S. Guo, S. Lv, H. Zhang, J. Ye, and P. Zhang, "Reflecting modulation," *IEEE J. Sel. Areas Commun.*, vol. 38, no. 11, pp. 2548–2561, Nov. 2020.

[14] M. K. Simon and M.-S. Alouini, *Digital Communication Over Fading Channels*, 2nd ed. New York, NY, USA: Wiley, 2005.

[15] Q. Li, M. Wen, E. Basar, and F. Chen, "Index modulated OFDM spread spectrum," *IEEE Trans. Wireless Commun.*, vol. 17, no. 4, pp. 2360–2374, Apr. 2018.